Maurya, Somendu; Nyman, Markus; Kaivola, Matti; Shevchenko, Andriy

Highly birefringent metamaterial structure as a tunable partial polarizer

Published in:
Optics Express

DOI:
10.1364/OE.27.027335

Published: 16/09/2019

Document Version
Publisher's PDF, also known as Version of record

Research Article | Vol. 27, No. 19 | 16 Sep 2019 | OPTICS EXPRESS 27335
Optics EXPRESS

Highly birefringent metamaterial structure as a tunable partial polarizer

SOMENDU MAURYA, MARKUS NYMAN, MATTI KAIVOLA, AND ANDRIY SHEVCHENKO*

Department of Applied Physics, Aalto University, P.O.Box 13500, FI-00076 Aalto, Finland
**andriy.shevchenko@aalto.fi*

Abstract: We consider a highly anisotropic metamaterial structure, composed of parallel metal nanostripes, and show that a thin layer of the material can be used as a tunable partial polarizer. The transmittance of the structure for TE-polarized waves depends strongly on the incidence angle, while for TM-polarized waves, it stays high and essentially constant. In particular, using the structure, the degree of polarization of a partially polarized or unpolarized light can be tuned by changing the incidence angle. The TE-wave transmittance drops from, c.a., 1 to 0 when the incidence angle increases by 5 deg only, owing to the presence of an unusual higher-order odd-symmetric TM mode that we have revealed in the structure. The tuning can be made smoother by introducing another layer of a similar metal-nanostripe structure on top of the first one. The new design allows the TE-wave transmittance to decrease gradually towards 0 with the incidence angle increasing from 0 to about 30 deg. Our structures serve as an essential optical component for studies involving partially polarized light.

1. Introduction

The polarization state of light plays a critical role in various phenomena of fundamental and applied physics, such as optical transitions between quantum states of atoms and molecules [1], absorption and scattering of light by nanoparticles [2], and reflection and transmission of electromagnetic waves at the boundaries between different materials [3]. Moreover, light polarization has found numerous technological applications, e.g., in optical communications [4], sensing [5], and imaging [6]. Even though the majority of these applications rely on completely polarized light, radiation from most natural and artificial light sources is partially polarized. Examples of partially polarized waves include light emitted by ordinary light bulbs and light emitting diodes, sun rays transmitted through the atmosphere, light from distant stars and planets, and even the cosmic microwave background radiation originating from the early Universe [7, 8]. The development of theoretical and experimental tools enabling the researchers to study and use partially polarized fields is of great scientific and technological importance [9].

Partially polarized light beams are characterized by their degree of polarization that determines the fraction of the polarized part of light in the beam. This parameter can be measured, e.g., by splitting the beam into its various linearly and circularly polarized components, measuring their intensities, and evaluating the beam Stokes parameters [10, 11]. Alternatively, one can use a technique based on the correlations of the beam intensity fluctuations [12–15], if the statistics of these fluctuations is known. In addition to the degree of polarization, one can measure the dynamical parameters of polarization fluctuations, such as the polarization time or the mean trajectory of the Poincare vector and its average deviations on the Poincare sphere [13, 16]. In all these measurements, a tunable partial polarizer that can control the transmission of one of the two orthogonal polarization components without affecting the other component would be a very useful tool.

Several approaches have been demonstrated to create and control partially polarized beams. For example, Lyot [17, 18] and double wedge [19] depolarizing systems can be applied to an

#372606 https://doi.org/10.1364/OE.27.027335
Journal © 2019 Received 15 Jul 2019; revised 8 Aug 2019; accepted 11 Aug 2019; published 13 Sep 2019

Optics EXPRESS

originally polarized beam to produce inhomogeneously polarized beams that on average can be considered as unpolarized. However, at each point in the transverse plane, the field is still fully polarized. A true depolarizer or a true partial polarizer can for example be obtained by using a Mach-Zehnder interferometer with polarizing beam splitters [20]. The device splits the beam into its orthogonal polarization components and makes them uncorrelated, as long as the length difference between the interferometer arms is larger than the coherence length of the beam field [16]. The transmittance of one of the arms can be made tunable, which will result in a tunable partial polarizer. This system, however, will be rather bulky and not very convenient, especially if the application requires rotation of the system around its optical axis.

In this work, we design a metamaterial structure able to act as a tunable partial polarizer that changes the intensity ratio between two orthogonal polarization components of the beam. The structure is a single layer of periodically arranged metal nanostripes designed to affect the two polarizations differently. The configuration is similar to that of a wire-grid polarizer [21–23], but its purpose is very different. Indeed, wire-grid polarizers operate in a cutoff regime for the transverse-electric wave component (polarized along the wires) to block it completely at all possible incidence angles. Our structure, in contrast, is highly transmissive for both transverse magnetic (TM) and transverse electric (TE) polarizations at normal incidence, and when the incidence angle increases, the transmittance of the TE component gradually decreases to zero while that of the TM component stays high. Hence, the metasurface can act as a tunable partial polarizer with the tunability provided by the adjustable incidence angle. We also show that by using two layers of similar metal nanostripes, one can make the tuning smoother and move the tunability region to smaller incidence angles. Our metamaterial-based devices have clear advantages over the devices based on tilted dielectric plates near the Brewster angle [24] (as the tunability range of these plates is small even in the presence of several interfaces) and tunable polarizers utilizing anisotropic absorption in graphene [25, 26] (as they operate at terahertz frequencies and in the reflection mode only). It is worth mentioning that, while many metamaterial and metasurface structures have been proposed and demonstrated to control light polarization [27–32], none of them have been designed to act as a tunable partial polarizer similar to our metamaterial-based component. We anticipate that the new type of an optical polarizer proposed in this work can become a part of many polarization-sensitive optical measurement setups and devices.

2. Theory and design

2.1. Tuning the degree of polarization

The degree of polarization of a partially polarized optical wave can be expressed as the ratio of the intensity of its polarized part to the total intensity of the wave [3], i.e.,

$$p = \frac{I_{\text{polarized}}}{I_{\text{total}}}. \tag{1}$$

If the wave is unpolarized, its orthogonal polarization components do not correlate and have equal intensities, i.e., $I_x = I_y$ for a wave propagating in the z-direction. The degree of polarization in this case is equal to 0. If one of the components becomes weaker in intensity, the degree of polarization increases in accordance with

$$p = \frac{|I_x - I_y|}{I_x + I_y}. \tag{2}$$

If one of the components vanishes, p becomes equal to 1. Hence, by controlling the intensity of one polarization component without affecting the other one, the degree of polarization can be tuned between 0 and 1. A tunable partial polarizer can be used to achieve this control. Moreover,

Optics EXPRESS

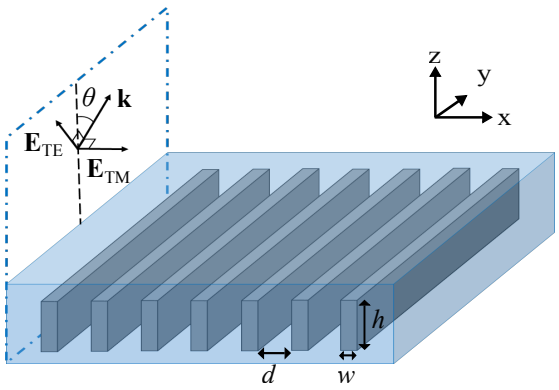

Fig. 1. Schematic of a layer of an anisotropic metamaterial composed of silver nanostripes in a dielectric medium. The width and separation distance of the nanostripes are w and d, respectively. The thickness of the metamaterial layer given by the height of the nanostripes is h.

using the same device, an arbitrary partially polarized beam can be made unpolarized. The polarized part of a partially polarized beam can be removed by the partial polarizer, thus setting $I_x - I_y = 0$. If the polarized part is elliptically polarized, then a quarter-wave plate can be used first to make this part linearly polarized. Such a wave plate can also be made in the form of a thin metamaterial layer [27].

2.2. Metamaterial design

A planar metamaterial structure that we propose is a periodic array of silver nanostripes embedded in a transparent dielectric medium (see Fig. 1). The width, height and separation of the nanostripes are w, h and d, respectively. We start by assuming that the height h of the stripes is infinite and calculate the effective refractive indices n_{TE} and n_{TM} for fundamental TE and TM modes of the structure using the following equations [33]:

$$\frac{\tan(\frac{1}{2}k_0 d\sqrt{\epsilon_{\mathrm{d}} - n_{\mathrm{TE}}^2})}{\tan(\frac{1}{2}k_0 w\sqrt{\epsilon_{\mathrm{m}} - n_{\mathrm{TE}}^2})} = -\frac{\sqrt{\epsilon_{\mathrm{m}} - n_{\mathrm{TE}}^2}}{\sqrt{\epsilon_{\mathrm{d}} - n_{\mathrm{TE}}^2}}, \tag{3}$$

$$\frac{\tan(\frac{1}{2}k_0 d\sqrt{\epsilon_{\mathrm{d}} - n_{\mathrm{TM}}^2})}{\tan(\frac{1}{2}k_0 w\sqrt{\epsilon_{\mathrm{m}} - n_{\mathrm{TM}}^2})} = -\frac{\epsilon_{\mathrm{d}}\sqrt{\epsilon_{\mathrm{m}} - n_{\mathrm{TM}}^2}}{\epsilon_{\mathrm{m}}\sqrt{\epsilon_{\mathrm{d}} - n_{\mathrm{TM}}^2}}. \tag{4}$$

Here, k_0 is the wavenumber in vacuum and ϵ_{m} and ϵ_{d} are the dielectric constants of the metal and the dielectric, respectively. The mode polarizations are shown in Fig. 1. We choose the metal to be silver and the dielectric to be glass with $\epsilon_{\mathrm{d}} = 2.25$. The refractive index of silver is taken from [34]. For the structure to operate at a wavelength of 780 nm, we select $w = 90$ nm and $d = 310$ nm and obtain $n_{\mathrm{TE}} \approx 1.0$ and $n_{\mathrm{TM}} \approx 1.6$. For a finite structure, at the glass-metamaterial interface, the TM mode must exhibit a high transmittance that is nearly independent of the incidence angle, while the transmittance of the TE mode should decrease when the incidence angle approaches the critical angle of total internal reflection $\theta_{\mathrm{c}} = \arcsin(n_{\mathrm{TE}}/n_{\mathrm{d}}) \approx 42$ deg. However, in the presence of the metamaterial-glass interface, a TE wave at a non-zero incidence angle can excite an additional higher-order mode in the metamaterial. This mode shows a non-zero x-component of the electric field originating from a periodic charge distribution in

Optics EXPRESS

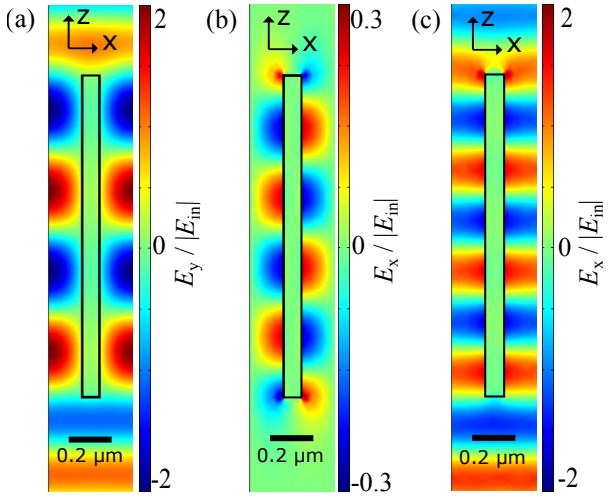

Fig. 2. Electric field profiles in the XZ plane of the structure for the incident TE- and TM-polarized waves for a 1.53 μm tall and 90 nm wide metal nanostripes: (a) shows the y-component of the excited TE mode in the structure when a TE-polarized plane wave is incident on it at normal incidence, (b) shows the x-component of the excited OTM mode when a TE-polarized wave is incident at an angle of 5 deg, and (c) shows the x-component of the excited TM mode for a TM-polarized incident wave at normal incidence.

the metal nanostripes along z. It is therefore an odd-symmetric (or anti-symmetric) transverse magnetic (OTM) mode with the refractive index n_{OTM} given by

$$\frac{\tan(\frac{1}{2}k_0 d\sqrt{\epsilon_{\mathrm{d}} - n_{\mathrm{OTM}}^2})}{\tan(\frac{1}{2}k_0 w\sqrt{\epsilon_{\mathrm{m}} - n_{\mathrm{OTM}}^2})} = -\frac{\epsilon_{\mathrm{m}}\sqrt{\epsilon_{\mathrm{d}} - n_{\mathrm{OTM}}^2}}{\epsilon_{\mathrm{d}}\sqrt{\epsilon_{\mathrm{m}} - n_{\mathrm{OTM}}^2}}. \tag{5}$$

Similarly to Eqs. (3) and (4), this equation has been derived by matching the fields at the metal-dielectric interface. For the considered structure, Eq. (5) gives $n_{\mathrm{OTM}} \approx 1.2$. The correctness of the evaluated mode indices was verified numerically using COMSOL Multiphysics. The numerically calculated field distributions of the three modes are illustrated in Fig. 2 for $h = 1.53$ μm. A distinctive feature of the higher-order OTM mode is that it has a low coupling efficiency to plane waves propagating in the substrate. As a result, it exhibits a high reflection coefficient at the metamaterial-glass interface and a high finesse when the mode satisfies the Fabry-Perot resonance condition inside the metamaterial layer. When $h = 200$ nm, the Fabry-Perot resonance for this mode takes place at $\theta = 13$ deg. For a finite h, all three modes undergo phase shifts upon reflection and transmission at the glass-metamaterial interface. These phase shifts, however, are not determined solely by the index contrast, but also include the contribution from plasmon excitations at the edges of the metal stripes and the near-field interaction effects between them. Furthermore, inside the material, upon reflection, part of the energy is transferred from TE to OTM mode of the structure and vice versa. Therefore, the multiple reflections of these modes in the metamaterial slab must be described in terms of the mode reflection and transmission matrices

$$\hat{\mathbf{r}} = \begin{pmatrix} r_{\text{TE-TE}} & r_{\text{TE-OTM}} \\ r_{\text{OTM-TE}} & r_{\text{OTM-OTM}} \end{pmatrix}, \tag{6}$$

Optics EXPRESS

$$\hat{\mathbf{t}} = \begin{pmatrix} t_{\mathrm{TE}} & t_{\mathrm{OTM}} \\ a & b \end{pmatrix}, \tag{7}$$

where r_{i-j} is the reflection coefficient for the mode j converted to the mode i upon reflection and t_j is the transmission coefficient of mode j of the structure to the TE-polarized plane wave in the surrounding medium. If the surrounding medium is a homogeneous dielectric, as in our case, the coefficients a and b in the transmission matrix are equal to zero, because the OTM mode remains evanescent outside the material. We have evaluated the reflection and transmission coefficients in Eqs. (6) and (7) numerically at the metamaterial-glass interface. In the analytical model, the incident wave vector with the complex amplitude of the electric field E_i is expressed in the basis of the TE and OTM modes as

$$\mathbf{E}_{\mathrm{i}} = \begin{pmatrix} E_{\mathrm{i}} \\ 0 \end{pmatrix}. \tag{8}$$

Since the incident wave has only a TE-polarized component, the second element of $\mathbf{E}_{\mathrm{i}}$ is equal to zero. The reflection and transmission matrices for the incident TE wave are expressed as

$$\hat{\mathbf{r}}_{\mathrm{i}} = \begin{pmatrix} r_{\mathrm{TE}} & 0 \\ 0 & r_{\mathrm{OTM}} \end{pmatrix}, \tag{9}$$

$$\hat{\mathbf{t}}_{\mathrm{i}} = \begin{pmatrix} t'_{\mathrm{TE}} & c \\ t'_{\mathrm{OTM}} & d \end{pmatrix}, \tag{10}$$

where t'_j is the transmission coefficient of the TE-polarized wave to mode j of the structure. The coefficients c and d are the transmission coefficients of the OTM mode in glass to the TE and OTM modes in the metamaterial which do not contribute to the field inside the metamaterial because the OTM mode does not exist in the incident field. The vector of the transmitted wave is calculated using the transfer matrix formalism of [35] as

$$\mathbf{E}_{\mathrm{t}} = \begin{pmatrix} E_{\mathrm{t,TE}} \\ E_{\mathrm{t,OTM}} \end{pmatrix}, \tag{11}$$

where

$$\mathbf{E}_{\mathrm{t}} = \hat{\mathbf{t}}[\mathbf{I} - \hat{\mathbf{p}}\hat{\mathbf{r}}\hat{\mathbf{p}}\hat{\mathbf{r}}]^{-1}\hat{\mathbf{p}}\hat{\mathbf{t}}_{\mathrm{i}}\mathbf{E}_{\mathrm{i}}. \tag{12}$$

Here, $\hat{\mathbf{p}}$ is the propagation matrix of the modes inside the metamaterial slab given in terms of the z-component of the wavevector k_z by

$$\hat{\mathbf{p}} = \begin{pmatrix} \exp(-ihk_{\mathrm{z,TE}}) & 0 \\ 0 & \exp(-ihk_{\mathrm{z,OTM}}) \end{pmatrix}. \tag{13}$$

The transmittance for the incident TE mode is then found from

$$T_{\mathrm{TE}} = \left| \frac{E_{\mathrm{t,TE}}}{E_{\mathrm{i}}} \right|^2. \tag{14}$$

Note that $E_{\mathrm{t,OTM}}$ would be equal to zero because transmission coefficients a and b for the OTM mode in Eq. (7) are equal to zero. For the incident TM-polarized wave, the transmittance T_{TM} is calculated using a standard expression for a Fabry-Perot resonator of a slab with a refractive index

Optics EXPRESS

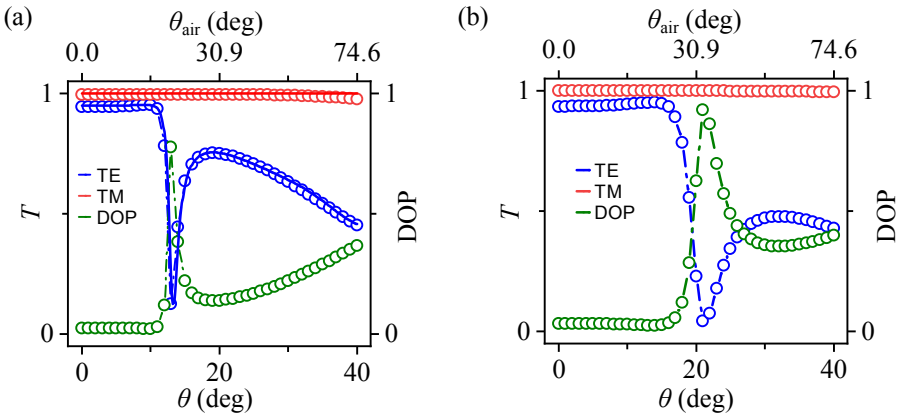

Fig. 3. The transmittance (T) of the designed metamaterial slab as a function of the incidence angle θ in glass and θ_{air} in air. The results of semianalytical calculations are shown by solid lines and those of purely numerical calculations by dashed lines and circles. The green curve shows the degree of polarization (DOP) of an initially unpolarized wave transmitted by the device. The dimensions of the structure are $h = 200$ nm and $d = 310$ nm. The width of the metal nanostripes is $w = 90$ nm in (a) and $w = 30$ nm in (b).

$n_{TM} = 1.62$, because the wave does not split into different modes during propagation through or surface reflections in the metamaterial.

Using the numerically calculated complex reflection and transmission coefficients obtained for the modes at the metamaterial-glass boundaries, we apply the above equations and calculate T_{TE} and T_{TM} of the metamaterial slab as functions of the incidence angle and obtain the curves shown in Fig. 3(a) (see the blue and red solid lines). The sharp decrease of T_{TE} at $\theta = 13$ deg is caused by destructive interference of the transmitted resonant OTM and TE modes. The transmittance of the TM wave, in contrast, remains close to 1 independently of the incidence angle. For comparison, the results of purely numerical calculations based on COMSOL Multiphysics are illustrated in Fig. 3 by circles. The two approaches give very similar results, verifying the correctness of our intuitive physical picture. The phase difference acquired by the TE and TM components upon transmission through the material is approximately equal to 0.5π at all the angles of incidence considered in the calculations, which can be of relevance in some cases dealing with initially polarized incident light. The green lines in Fig. 3 show the degree of polarization of an initially unpolarized light transmitted by the structure as a function of θ. If the structure is embedded in a parallel glass plate, the incidence angle in air, θ_{air}, is larger than θ. This angle is also shown in the figure.

The position of the dip in the curve $T_{TE}(\theta)$ can be tuned by tuning the geometrical parameters of the structure. For example, for metal nanostripes with a smaller width, the dip appears at larger angles. Figure 3(b) shows the transmittance curves calculated for the case of $w = 30$ nm. The degree of polarization of an unpolarized incident light beam can now be tuned by changing the incident angle from 15 to 21 deg. We keep the separation between the stripes the same, which makes the period of the structure equal to 340 nm. It is interesting to note that now the phase difference of the TE and TM waves gained in the transmission through the material is about 0.8π. In principle, if needed, it can be set to a desired value by adjusting the dimensions for the structure.

Optics EXPRESS

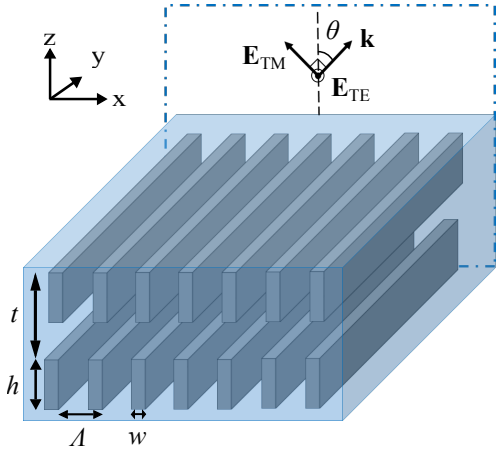

Fig. 4. A bi-layered metamaterial structure. The center-to-center separation of the layers is t. Each layer is composed of an array of silver nanostripes of height h and width w. The period of the structure is Λ. The incident wavevector lies in the XZ plane and makes an angle θ with the z-axis.

2.3. Bi-layered metamaterial

The transmittance of a TE wave through the metamaterial structure described above is extremely sensitive to the incidence angle in the range of the OTM-mode resonance, which can be a problem, e.g., if the transmittance has to be tuned with high precision. The second structure that we propose has a much lower angle sensitivity. It contains two metamaterial layers, as shown in Fig. 4. Each of the layers acts as a polarization-sensitive mirror and the whole structure is in essence a Fabry-Perot resonator. Figure 5 shows the dependence of the reflectance of a single layer of the structure on dimensions h and w with a fixed period $\Lambda = 200$ nm. The period is chosen such that the TE-polarized light at $\lambda_0 = 780$ nm is in the cutoff regime with both TE and OTM modes inside the layer. We see that the reflectance for TM-polarized light depends mainly on the width of the metal nanostripes, while the reflectance of TE-polarized light depends on the cross-sectional area ($\sigma = hw$) of the stripes. For large σ, the metamaterial slab acts as a wire grid polarizer. Using two such metamaterial layers, we can form a Fabry-Perot resonator with different reflection coefficients for the incident TE- and TM-polarized waves. In particular, we expect the resonator to be highly transmitting for TM-polarized waves at all incidence angles. Simultaneously, for TE-polarized waves that show high single layer reflectivity, the resonator transmittance must depend on the incidence angle, because the Fabry-Perot resonance condition depends on this angle.

The dimensions chosen for our design are $h = 100$ nm and $w = 40$ nm, which gives the reflectances of TE- and TM-polarized waves to be 57% and 2%, respectively, at normal incidence (Figs. 5(a) and 5(b)). The distance $t = 740$ nm is chosen to obtain a Fabry-Perot resonance for TE polarized light at normal incidence ($\theta = 0$) and maximize the transmittance of the device. Figure 5(c) shows the transmittance of the device as a function of distance t at $\lambda_0 = 780$ nm. Then, when θ increases, the resonator becomes off-resonant and the transmission decreases. The numerically calculated angle-dependent transmittance of the structure for TE- and TM-polarized light are shown in Fig. 5(d) by the blue and red curves, respectively. The transmittance of TE-polarized light decreases from 95% to 5% as the incidence angle increases from 0 to 30 deg. The transmittance of TM-polarized light remains high at all incidence angles as expected. The on-resonance transmittance values are lower than 100% because of a non-negligible absorption loss in the structure. The green curve in the figure shows the degree of polarization of an initially

Optics EXPRESS

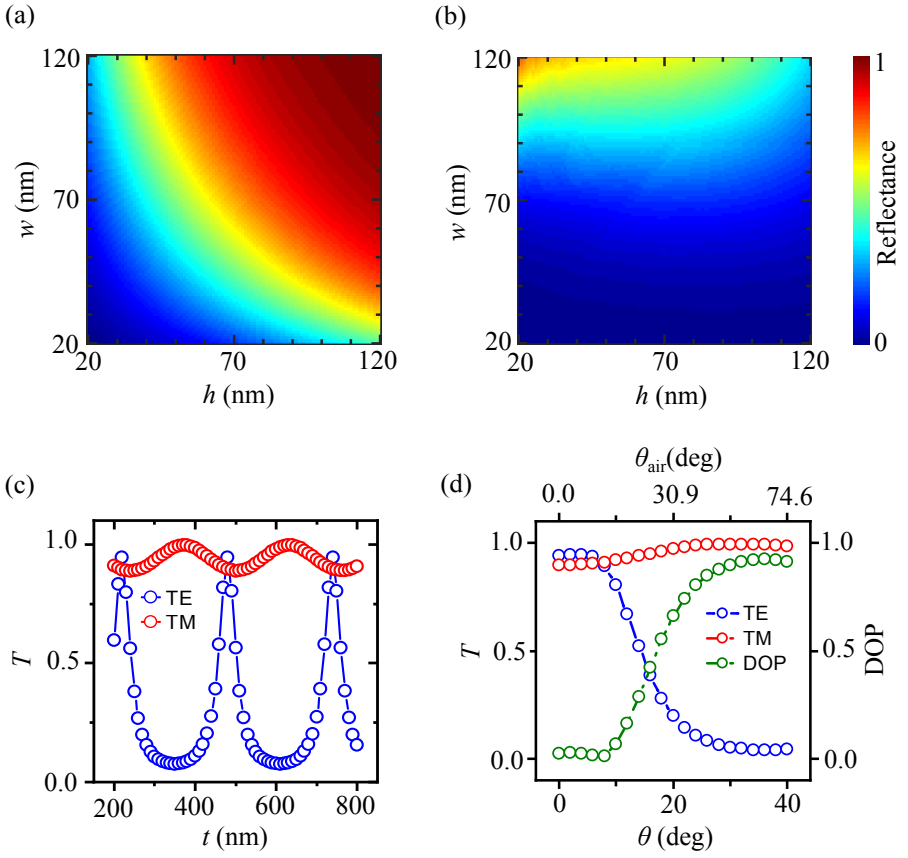

Fig. 5. Dependence of the reflectance of a single metamaterial layer with Λ =200 nm for normally incident (a) TE-polarized and (b) TM-polarized waves on parameters h and w. The transmittance of the bi-layered metamaterial (h = 100 nm and w = 40 nm) for the incident TE-polarized and TM-polarized waves is shown by the blue and red lines, respectively, in (c) as a function of size t and in (d) as a function of the incidence angle at t = 740 nm. The degree of polarization (DOP) of originally unpolarized light transmitted by the device is shown by the green curve in (d).

unpolarized wave transmitted by the device. The degree of polarization is seen to smoothly increase from 0 to 0.9 when the incidence angle increases from 0 to 30 deg.

For convenience in practical applications, the designed partial polarizer can be attached to a mount that can be rotated and tilted. By rotating it around the optical axis, one can choose the directions for the TE and TM polarization components of the light. The amplitudes of these components are then controlled by tilting. Such a device can be used either to tune or measure the degree of polarization of partially polarized optical waves.

3. Conclusions

We have theoretically analyzed a highly birefringent metamaterial structure made of parallel metal stripes in a dielectric host medium and found that, under certain conditions, a slab of such a material can support an unusual higher-order odd-symmetric TM mode. This mode, being only weakly coupled to external plane waves, shows a sharp resonance feature that, for TE-polarized

Optics EXPRESS

incident light, leads to a high sensitivity of the material's response to the incidence angle. Using the revealed properties of the material, we have designed two metamaterial structures that can be exploited as tunable partial polarizers. The tunability is based on the angle of incidence, which makes the device easy to use in experiments. The sensitivity of the first of the proposed structures to the incidence angle is high, which can find applications also in optical sensors or modulators. The second structure, with a lower sensitivity, can be more convenient for precise tuning or exact measurement of the degree of polarization of partially polarized optical beams. While the presented designs are optimized for a wavelength of 780 nm, it is easy to change the operation wavelength by changing the structure parameters. Due to simplicity of the design we expect that large-scale fabrication of the proposed structures is possible using nanoimprint or optical interference lithography.

Funding

Academy of Finland (308394); Finnish Cultural Foundation (00170774)

References

1. C. N. Banwell and E. M. McCash, *Fundamentals of Molecular Spectroscopy*, European Chemistry Series (McGraw-Hill, 1994).
2. C. F. Bohren and D. R. Huffman, *Absorption and Scattering of Light by Small Particles*, Wiley Science Series (Wiley, 2008).
3. B. Saleh and M. Teich, *Fundamentals of Photonics*, Wiley Series in Pure and Applied Optics (Wiley, 2007).
4. G. D. VanWiggeren and R. Roy, "Communication with dynamically fluctuating states of light polarization," Phys. Rev. Lett. **88**, 097903 (2002).
5. J. S. Tyo, D. L. Goldstein, D. B. Chenault, and J. A. Shaw, "Review of passive imaging polarimetry for remote sensing applications," Appl. Opt. **45**, 5453–5469 (2006).
6. K. Zhanghao, J. Gao, D. Jin, X. Zhang, and P. Xi, "Super-resolution fluorescence polarization microscopy," J. Innov. Opt. Heal. Sci. **11**, 1730002 (2018).
7. T. W. Cronin and J. Marshall, "Patterns and properties of polarized light in air and water," Philos. Transactions Royal Soc. B: Biol. Sci. **366**, 619–626 (2011).
8. S. Trippe, "Polarization and polarimetry: a review," J. Korean Astron. Soc. **47**, 15–39 (2014).
9. D. E. Aspnes, "Photometric ellipsometer for measuring partially polarized light," J. Opt. Soc. Am. **65**, 1274–1278 (1975).
10. R. M. A. Azzam, "Stokes-vector and mueller-matrix polarimetry," J. Opt. Soc. Am. A **33**, 1396–1408 (2016).
11. N. A. Rubin, A. Zaidi, M. Juhl, R. P. Li, J. B. Mueller, R. C. Devlin, K. Leósson, and F. Capasso, "Polarization state generation and measurement with a single metasurface," Opt. Express **26**, 21455–21478 (2018).
12. W. H. Carter and E. Wolf, "Degree of polarization and intensity fluctuations in thermal light beams," J. Opt. Soc. Am. **63**, 1619–1620 (1973).
13. T. Setälä, A. Shevchenko, M. Kaivola, and A. T. Friberg, "Polarization time and length for random optical beams," Phys. Rev. A **78**, 033817 (2008).
14. A. Shevchenko, T. Setälä, M. Kaivola, and A. T. Friberg, "Characterization of polarization fluctuations in random electromagnetic beams," New J. Phys. **11**, 073004 (2009).
15. T. Voipio, T. Setälä, A. Shevchenko, and A. T. Friberg, "Polarization dynamics and polarization time of random three-dimensional electromagnetic fields," Phys. Rev. A **82**, 063807 (2010).
16. A. Shevchenko, M. Roussey, A. T. Friberg, and T. Setälä, "Polarization time of unpolarized light," Optica **4**, 64–70 (2017).
17. A. P. Loeber, "Depolarization of white light by a birefringent crystal. ii. the lyot depolarizer," J. Opt. Soc. Am. **72**, 650–656 (1982).
18. J. S. Wang, J. R. Costelloe, and R. H. Stolen, "Reduction of the degree of polarization of a laser diode with a fiber lyot depolarizer," IEEE Photonics Technol. Lett. **11**, 1449–1451 (1999).
19. J. C. G. de Sande, M. Santarsiero, G. Piquero, and F. Gori, "Longitudinal polarization periodicity of unpolarized light passing through a double wedge depolarizer," Opt. Express **20**, 27348–27360 (2012).
20. A. S. Ostrovsky, G. R. Zurita, C. M. Fabián, M. A. O. Santamaría, and C. R. Parrao, "Experimental generating the partially coherent and partially polarized electromagnetic source," Opt. Express **18**, 12864–12871 (2010).
21. J. J. Wang, W. Zhang, X. Deng, J. Deng, F. Liu, P. Sciortino, and L. Chen, "High-performance nanowire-grid polarizers," Opt. Lett. **30**, 195–197 (2005).
22. Z. Yang and Y. Lu, "Broadband nanowire-grid polarizers in ultraviolet-visible-near-infrared regions," Opt. Express **15**, 9510–9519 (2007).
23. J. W. Yoon, K. J. Lee, and R. Magnusson, "Ultra-sparse dielectric nanowire grids as wideband reflectors and polarizers," Opt. Express **23**, 28849–28856 (2015).

Optics EXPRESS

24. E. Compain and B. Drevillon, "High-frequency modulation of the four states of polarization of light with a single phase modulator," Rev. Sci. Instruments **69**, 1574–1580 (1998).
25. Y. V. Bludov, M. I. Vasilevskiy, and N. M. R. Peres, "Tunable graphene-based polarizer," J. Appl. Phys. **112**, 084320 (2012).
26. A. Fallahi and J. Perruisseau-Carrier, "Design of tunable biperiodic graphene metasurfaces," Phys. Rev. B **86**, 195408 (2012).
27. M. Nyman, S. Maurya, M. Kaivola, and A. Shevchenko, "Optical wave retarder based on metal-nanostripe metamaterial," Opt. Lett. **44**, 3102–3105 (2019).
28. S. M. Kamali, E. Arbabi, A. Arbabi, and A. Faraon, "A review of dielectric optical metasurfaces for wavefront control," Nanophotonics **7**, 1041–1068 (2018).
29. S.-E. Mun, J. Hong, J.-G. Yun, and B. Lee, "Broadband circular polarizer for randomly polarized light in few-layer metasurface," Sci. Reports **9**, 2543 (2019).
30. B. Shen, P. Wang, R. Polson, and R. Menon, "Ultra-high-efficiency metamaterial polarizer," Optica **1**, 356–360 (2014).
31. D. L. Markovich, A. Andryieuski, M. Zalkovskij, R. Malureanu, and A. V. Lavrinenko, "Metamaterial polarization converter analysis: limits of performance," Appl. Phys. B **112**, 143–152 (2013).
32. H. Kurosawa, B. Choi, Y. Sugimoto, and M. Iwanaga, "High-performance metasurface polarizers with extinction ratios exceeding 12000," Opt. Express **25**, 4446–4455 (2017).
33. Y. Pang and R. Gordon, "Metal nano-grid reflective wave plate," Opt. Express **17**, 2871–2879 (2009).
34. P. B. Johnson and R. W. Christy, "Optical constants of the noble metals," Phys. Rev. B **6**, 4370–4379 (1972).
35. V. Kivijärvi, M. Nyman, A. Karrila, P. Grahn, A. Shevchenko, and M. Kaivola, "Interaction of metamaterials with optical beams," New J. Phys. **17**, 063019 (2015).